Femtosecond 1*P*-to-1*S* Electron Relaxation in Strongly Confined Semiconductor Nanocrystals

Victor I. Klimov* and Duncan W. McBranch

Chemical Sciences and Technology Division, CST-6, MS-J585, Los Alamos National Laboratory, Los Alamos, New Mexico 87545

(Received 21 October 1997)

High-sensitivity femtosecond transient absorption is applied to directly measure the population-depopulation dynamics of the lowest ($1S$) and the first excited ($1P$) electron states in CdSe nanocrystals (NC's) of different radii with $1S$—$1P$ energy separation up to 16 longitudinal optical phonon energies. Instead of the drastic reduction of the energy relaxation rate expected due to a phonon bottleneck, we observe a fast subpicosecond $1P$-to-$1S$ relaxation, with the rate enhanced in NC's of smaller radius. This indicates the opening of new confinement-enhanced relaxation channels which likely involve Auger-type electron-hole energy transfer. [S0031-9007(98)06020-7]

PACS numbers: 73.20.Dx, 42.70.Nq, 78.47.+p

Semiconductor nanocrystals (NC's) or quantum dots (QD's) exhibit a number of novel physical properties not observable in bulk materials [1,2]. Because of the discrete energy spectrum resulting from three-dimensional (3D) confinement, the carrier energy relaxation dynamics in NC's are significantly different from those in systems with continuous energy spectra. Even in the regime of weak confinement when the level spacing is only a few meV, the carrier relaxation mediated by interactions with phonons is hindered dramatically, because of restrictions imposed by energy and momentum conservation ("phonon bottleneck") [3,4]. Further reduction in the energy loss rate is expected in the regime of strong confinement, for which the level spacing can greatly exceed typical phonon energies, and hence carrier-phonon scattering can occur only via weak multiphonon processes [5].

Experimental studies on energy relaxation in 3D-confined systems have concentrated on III-V QD's made by epitaxial techniques [6–9]. Several groups reported observations of a phonon bottleneck in these structures [6,7]. However, other studies [8–10] indicate that energy relaxation in QD's is not significantly slower than in materials with continuous energy spectra. Such mechanisms as Auger-type scattering in the presence of dense electron-hole (e-h) plasmas [11], Auger-like electron-hole energy transfer [12], and defect-mediated relaxation [13] have been proposed to explain a possible breakdown of phonon bottleneck in QD's.

The interpretation of energy relaxation in epitaxially grown QD's is complicated by a large number of defects (introduced, e.g., during lateral patterning) and the complex structure of the samples, which in addition to 0D regions contain also optically active bulk and 2D regions. An alternative approach to making high quality QD's is by chemical synthesis based on the control of homogeneous nucleation which allows preparation of NC's with well passivated surfaces and size dispersion less than 5% [14]. These NC's can be dissolved in a variety of transparent organic solvents, or incorporated into optically passive polymer or glass matrices. In contrast to epitaxially grown QD's with relatively large lateral dimensions (typically greater than 10 nm), the size of chemically synthesized NC's can be easily tuned into the sub-10-nm range, allowing one to study the regime of very strong confinement, for which interlevel relaxation by direct phonon emission can be explicitly ruled out.

For either epitaxial or chemically prepared QD's, there have been no previous direct measurements of relaxation between adjacent quantized states with femtosecond (fs) time resolution. In this Letter, we report fs transient absorption (TA) studies of intraband relaxation in CdSe NC's with mean radii (R) from 2 to 5.6 nm. For these sizes, the spacing between the two lowest electron levels is in the range of $4-16\ \hbar\omega_0$ [$\hbar\omega_0$ is the energy of the longitudinal optical (LO) phonon]. We extract complementary population dynamics of the lowest ($1S$) and the first excited ($1P$) electron states. Our data indicate that even in NC's for which the $1P$–$1S$ energy spacing is as large as $16\ \hbar\omega_0$, the $1P$-to-$1S$ relaxation is characterized by an extremely short time constant of ~300 fs. The $1S$-state buildup time *decreases* for NC of smaller radius, indicating a *confinement-induced enhancement* in the relaxation rate.

To probe carrier dynamics, we monitored carrier-induced absorption changes using a fs pump-probe experiment in the novel chirp-free configuration (accuracy up to 10^{-5} in differential transmission) [15]. The samples were pumped at 3.1 eV by frequency-doubled 100-fs pulses from an amplified Ti-sapphire laser. The transmission of the photoexcited spot was probed by variably delayed pulses of a white light fs continuum. To exclude the effect of many-particle interactions on relaxation dynamics, the pump fluence was kept below 25 $\mu J\,cm^{-2}$, corresponding to excitation of less than one e-h pair per NC on average. All measurements were performed at room temperature. Two different types of samples were studied: CdSe NC/glass composites prepared by high-temperature precipitation [16] and CdSe colloidal NC's made by a template-directed synthesis in an inverse-micelle solution [14]. The size dispersion was (10–15)% in glass samples and less than 5% in colloids.

 0031-9007/98/80(18)/4028(4)$15.00

The nonlinear optical response in NC's is typically dominated by state filling [17,18] leading to pronounced bleaching bands at energies of the allowed optical transitions. Because of degeneracy of the valence band and a large difference between electron and hole masses in CdSe ($m_h/m_e \approx 6$), the bleaching bands at room temperature are dominated by the electron populations [19]. TA signals are also affected by Coulomb effects due to two e-h-pair interactions (biexciton effect) [20,21] and the trapped-carrier-induced dc-Stark effect [22,23]. While state filling affects only transitions coupling populated states, the Coulomb interaction influences all transitions in NC's, resulting in transition shifts which are seen as derivativelike features in TA spectra [20–23]. To extract carrier dynamics from TA data, the state-filling-induced portion of the TA must be accurately separated from contributions due to Coulomb effects.

Figure 1 shows the short-term dynamics of the pump-induced absorption changes ($\Delta\alpha d$; d is a sample thickness) for glass [(a), $R = 4.2$ nm] and colloidal [(b), $R = 2.3$ nm] samples with $1S$-$1P$ energy separations of ~6 and ~14 LO phonon energies, respectively. At probe delay times $\Delta t \geq 1$ ps, in both samples, the TA is dominated by two bleaching bands B_1 and B_2. B_1 marks the position of the lowest $1S(e)$-$1S_{3/2}(h)$ transition (the $1S$ transition) between electron and hole quantized states. The high-energy bleaching (B_2) is separated from B_1 by ~400 meV which is close to the valence band spin-orbit splitting in bulk CdSe (420 meV). This allows us to assign the B_2 band to the transition coupling the $1S$ electron state to the hole state $2S_{1/2}$ ($R = 2.3$ nm) or $3S_{1/2}$ ($R = 4.2$ nm) [24] originating from the spin-orbit split-off valence subband. The B_2 band also contains contributions from spectrally close transitions as discussed below.

At sub-ps probe delay times, in both samples we see a pronounced derivativelike feature at the position of the $1S$ transition. With increasing Δt, the negative lobe of this feature (B_1) grows in, accompanied by a complementary decay of the positive lobe (A_1 in Fig. 1). At $\Delta t <$ 500 fs, the TA spectra of the glass sample [Fig. 1(a)] show an additional short-lived bleaching band (B_3) at ~2 eV. The position of this band is consistent with the energy of the $1P(e)$-$1P_{3/2}(h)$ transition (the $1P$ transition) [24]. Therefore, the B_3-band dynamics can be related to population changes of the $1P$ electron state.

The decay of B_3 [Fig. 2(a), open squares] is extremely fast (320-fs time constant) which we attribute to the depopulation of the $1P$ state. The $1S$ time transient [solid circles in Fig. 2(a)] shows a fast initial rise, followed by a clearly resolved step at ~200 fs, and a slower signal increase (time constant of ~300 fs) which is complementary to the B_3 decay. The two different contributions to B_1 can be explained in terms of Coulomb two-pair interactions and state filling, which is confirmed by modeling of time-resolved TA spectra assuming carrier redistribution between the $1P$ and $1S$ electron states [20] [see inset to Fig. 1(a)]. The step in the B_1 time transient is an unmistakable signature of different time offsets for these contributions. The Coulomb interaction leads to an instantaneous redshift of the $1S$ transition following photoexcitation. This results in a positive TA signal at A_1 and the initial fast onset of B_1, with buildup dynamics almost identical to those of B_3 [Fig. 2(a)]. The delayed growth of B_1 is due to increasing population of the $1S$ state as a result of carrier relaxation from the $1P$ state, consistent with the complementary decay of B_3 due to the depopulation of the $1P$ state. Because of a large bandwidth of optical transitions, the increasing bleaching of the $1S$ transition overwhelms the positive TA feature below B_1, resulting in the matching dynamics of B_3 and A_1 [Fig. 2(a)]. The sub-ps buildup of the $1S$ bleaching measured by us is consistent with previous observations of ultrafast $1S$ dynamics in glass samples doped with II-VI NC's [18,25,26].

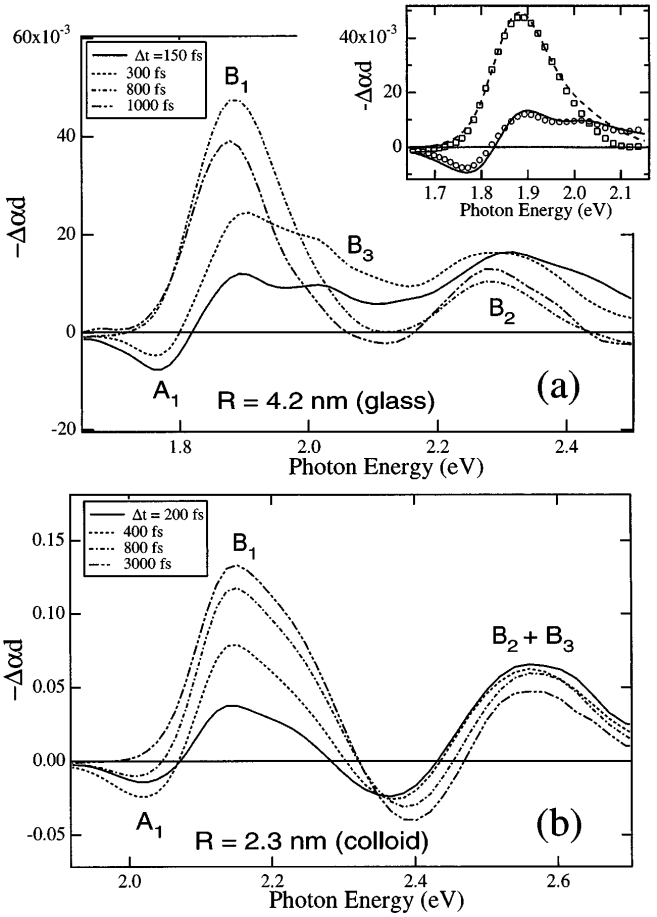

FIG. 1. Chirp-free TA spectra recorded at different delay times between pump and probe pulses for glass (a) and colloidal (b) samples with average radii 4.2 and 2.3 nm, respectively. Inset: TA spectra measured at 150 fs (circles) and 800 fs (squares) after excitation in comparison to calculations assuming that NC's are populated either in the $1P$ (solid line) or $1S$ (dashed line) states.

A similar analysis of TA can be performed for colloidal NC's as illustrated in Fig. 2(b) for the sample with

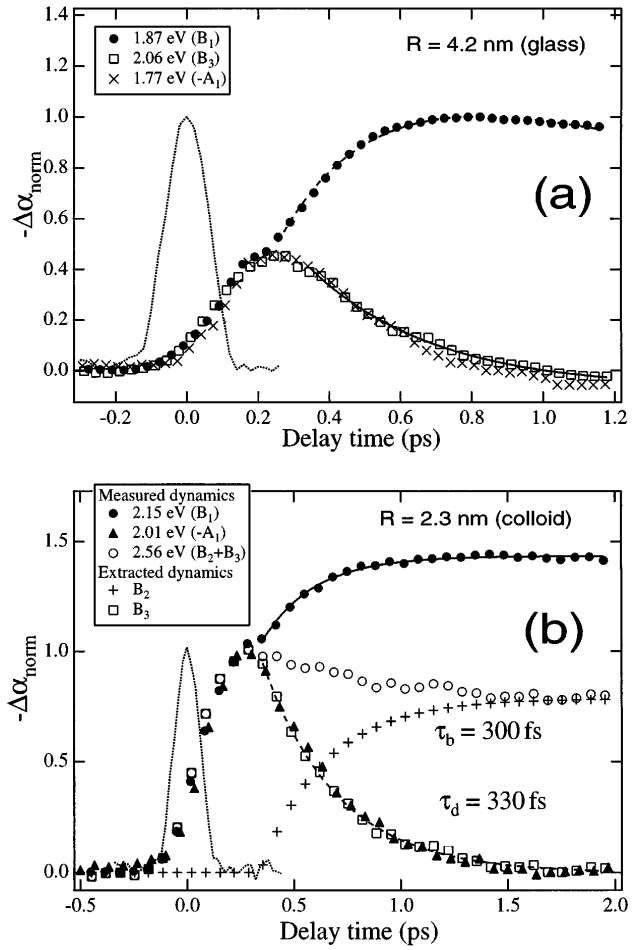

FIG. 2. (a) Normalized dynamics of the B_1 (solid circles), B_3 (open squares), and A_1 (crosses) TA features in the glass sample with $R = 4.2$ nm. Lines are fits assuming the $1P$-to-$1S$ relaxation time of 320 fs. (b) Normalized dynamics of the B_1 (solid circles), $B_2 + B_3$ (open circles), and A_1 (solid triangles) TA features in the colloidal sample with $R = 2.3$ nm. Solid line is a fit to a 300-fs exponential growth, dashed line is a fit to a 330-fs exponential decay. The open squares show the dynamics of the $1P$ electron state extracted from the $(B_2 + B_3)$-band dynamics assuming an exponential population buildup of the $1S$ electron state with a time constant of 300 fs (crosses). The dotted line is the pump-probe cross correlation.

$R = 2.3$ nm. Because of increased level separation, this sample, in addition to the $1S$ transition (B_1), also exhibits a transition $1S(e)$-$2S_{3/2}$ [shoulder at ~2.21 eV; Fig. 1(b)] involving the first excited hole state [24]. The B_1 time transient shows a biexciton-effect induced fast rise (solid circles), followed by a step and a second growth (time constant ~300 fs) due to increasing population of the $1S$ state. These dynamics are complementary to the decay of A_1 (solid triangles) associated with the transition shift, as in the glass sample. In the TA spectra of the colloidal sample [Fig. 1(b)], the band associated with the $1P$ transition overlaps with the band due to $1S(e)$-$2S_{1/2}(h)$ transition [24]. Therefore the bleaching at 2.56 eV [$B_2 + B_3$ in Fig. 1(b)] is due to populations of both the $1S$ and $1P$ states. The dynamics of this band indeed show two different components: a fast and a slow one [Fig. 2(b), open circles]. Assuming that the slow component is due to the buildup of the $1S$ state, we can approximate it by an exponential growth with a time constant of 300 fs [crosses in Fig. 2(b)], as derived from the second-step dynamics of B_1. Subtracting this component from the 2.56-eV signal we obtain the dynamics related entirely to population changes of the $1P$ state [open squares in Fig. 2(b)]. As in the glass samples, these dynamics closely match those of A_1 [solid triangles in Fig. 2(b)]. A fit to the decay of the extracted B_3 signal gives a relaxation constant of 330 fs, close the secondary buildup time of B_1.

Our data indicate that the initial TA dynamics are quite similar in both colloidal and glass samples. For example, for colloidal NC's with $R = 4.1$ nm we deduce a $1S$-population time of ~400 fs, close to the ~300 fs measured for the glass sample with $R = 4.2$ nm [see Fig. 2(a)]. This demonstrates a negligible role of surface effects and lattice imperfections on the initial energy relaxation process.

The measured relaxation constants indicate a very high energy-loss rate: e.g., ~1.2 eV ps^{-1} in NC's with $R = 2.3$ nm. This value is almost a factor of 2 greater than the estimated rate for the unscreened polar interaction in bulk CdSe with a continuous energy spectrum, and many orders of magnitude higher than the relaxation rate expected for multiphonon processes [5]. Recent works have suggested that coupling to defects [13] and/or Auger-type interactions [11,12] can lead to fast energy relaxation not limited by phonon bottleneck. The first of these mechanisms suggests a sequential relaxation involving an electron transition to the defect, defect relaxation, and then transition back to the lower QD level. This scenario is obviously not consistent with measured complementary dynamics of the $1P$ and $1S$ states, indicating a direct $1P$-to-$1S$ electron transition. Another nonphonon relaxation mechanism [11] involves the Auger-type energy transfer from the electron to high density e-h plasmas (2D plasmas from the adjacent quantum well in Ref. [11]). However, this effect cannot be operative under our experimental conditions of low excitation densities (less than one e-h pair per NC) and with NC's dispersed in an insulating, optically transparent host. Most likely, the observed fast dynamics can be explained in terms of the Auger mechanism proposed in Ref. [12], which involves *confinement-enhanced energy transfer of the electron excess energy to a hole*, with subsequent fast hole relaxation through its dense spectrum of states.

The important role of confinement in the enhancement of the energy relaxation is evident from a comparison of the $1S$ state population dynamics in NC's of different radii (see Fig. 3), indicating *a decrease in the 1S buildup time (τ_b) with decreasing NC radius*. In the inset to Fig. 3 we summarize the relaxation data for seven different samples. These data show that τ_b shortens from ~900 fs for $R = 5.6$ nm to ~300 fs for $R = 2$ nm. The observed

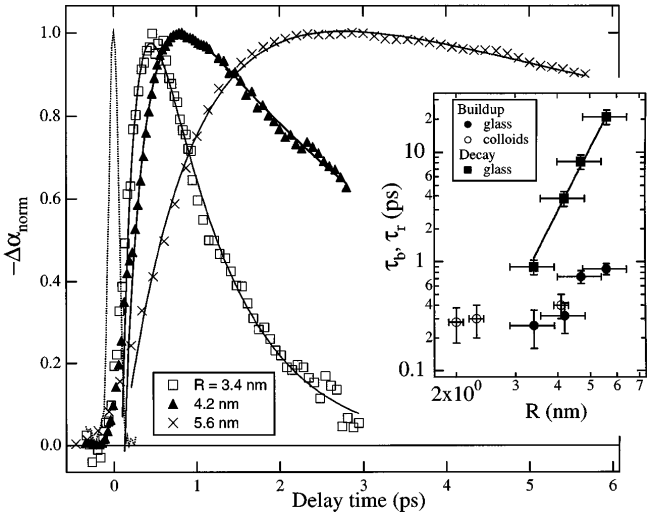

FIG. 3. Normalized dynamics of the $1S$ bleaching (band B_1) for three glass samples with NC radii 3.4 (open squares), 4.2 (solid triangles), and 5.6 nm (crosses) in comparison to fitting curves (solid lines) calculated for an exponential growth followed by an exponential decay. The time constants derived from these fits are shown in the inset along with data points for four other samples. The dotted line is the pump-probe cross correlation. Inset: Size dependence of the buildup (open and solid circles) and relaxation (solid squares) times of the $1S$ bleaching (band B_1). Relaxation times are shown only for glass samples, whereas buildup times are shown for both colloidal (open circles) and glass (solid circles) samples. The line is a fit to the R^6 dependence.

size dependence is exactly the opposite to that expected for phonon-dominated relaxation.

In contrast to the initial short-term dynamics which are similar in colloidal and glass samples, the long-term dynamics after relaxation to the lowest quantized states are strongly sample dependent. The B_1 decay in colloidal samples is characterized by a relaxation constant (τ_r) of 2–3 ns which can be assigned to the intrinsic radiative decay. In glass samples, the decay of the $1S$ bleaching occurs on a much faster ps time scale, with τ_r much shorter for NC's of smaller radius [see Fig. 3 inset (squares)] which is likely due to efficient trapping at deep defect states [27]. The observed size dependence ($\tau_r \propto R^6$; see inset to Fig. 3) can be explained in terms of confinement-induced squeezing of the $1S$ electron wave function, resulting in an increased overlap with the wave function of the deep-trap state [28].

In conclusion, we have performed direct measurements of the population-depopulation rates of the $1S$ and $1P$ electron states in semiconductor NC's with $1S$-$1P$ energy separation up to ~16 LO phonon energies. We observe a sub-ps $1P$-to-$1S$ energy relaxation, enhanced in NC's of smaller radius, which directly contradicts predictions for multiphonon emission. This suggests the opening of new confinement-enhanced relaxation channels which likely involve Auger-type electron-hole energy transfer. We observe similar initial energy relaxation in glass and colloidal samples, indicating a negligible role of surface/interface properties on the intraband relaxation process.

We thank M. Bawendi for providing high-quality colloidal samples, and Al. L. Efros for stimulating discussions. This research was supported by Los Alamos Directed Research and Development funds.

*Electronic address: klimov@lanl.gov

[1] L. Brus, Appl. Phys. A **53**, 465 (1991).
[2] A. P. Alivisatos, Science **271**, 933 (1996).
[3] U. Bockelmann and G. Bastard, Phys. Rev. B **42**, 8947 (1990).
[4] H. Benisty *et al.*, Phys. Rev. B **44**, 10 945 (1991).
[5] T. Inoshita and H. Sakaki, Phys. Rev. B **46**, 7260 (1992).
[6] K. Brunner *et al.*, Phys. Rev. Lett. **69**, 3216 (1992).
[7] T. H. Groerer *et al.*, Phys. Rev. B **53**, 16 474 (1996).
[8] B. Ohnesorge *et al.*, Phys. Rev. B **54**, 11 532 (1996).
[9] S. Grosse *et al.*, Phys. Rev. B **55**, 4473 (1997).
[10] N. Kirstaeder *et al.*, Electron. Lett. **30**, 1416 (1994).
[11] U. Bockelmann and T. Egler, Phys. Rev. B **46**, 15 574 (1992).
[12] Al. L. Efros, V. A. Kharchenko, and M. Rosen, Solid State Commun. **93**, 281 (1995).
[13] P. C. Sercel, Phys. Rev. B **51**, 14 532 (1995).
[14] C. B. Murray *et al.*, J. Am. Chem. Soc. **115**, 8706 (1993).
[15] V. Klimov and D. McBranch, Opt. Lett. **23**, 277 (1998).
[16] A. I. Ekimov and A. A. Onushenko, JETP Lett. **40**, 1136 (1984).
[17] V. Klimov, S. Hunsche, and H. Kurz, Phys. Status Solidi B **188**, 259 (1995).
[18] U. Woggon *et al.*, Phys. Rev. B **54**, 17 681 (1996).
[19] S. Hunsche *et al.*, Appl. Phys. B **62**, 3 (1996).
[20] V. Klimov, S. Hunsche, and H. Kurz, Phys. Rev. B **50**, 8110 (1994).
[21] K. I. Kang *et al.*, Phys. Rev. B **48**, 15 449 (1993).
[22] D. J. Norris *et al.*, Phys. Rev. Lett. **72**, 2612 (1994).
[23] V. Klimov and D. McBranch, Phys. Rev. B **55**, 13 173 (1997).
[24] D. J. Norris and M. G. Bawendi, Phys. Rev. B **53**, 16 338 (1996).
[25] K. Shum *et al.*, Phys. Rev. Lett. **68**, 3904 (1992).
[26] V. Klimov, P. Haring Bolivar, and H. Hurz, Phys. Rev. B **53**, 1463 (1996).
[27] N. Chesnoy *et al.*, J. Phys. Chem. **90**, 3393 (1986).
[28] Al. L. Efros (private communication).